

**ORIGINAL ARTICLE** 

**Submission:** 15/06/2024 **Accepted:** 22/09/2024

# SPATIOTEMPORAL VARIABILITY ANALYSIS OF WEATHER PARAMETERS IN CHITTAGONG CITY CORPORATION, BANGLADESH FROM 1990 TO 2020

Biswajit NATH<sup>1\*</sup> Sharif Md. Amirul ALAM<sup>1</sup> Md. Sayem AHMMED RIPON<sup>1</sup> Nasreen AKTER<sup>1</sup>

#### **ABSTRACT**

The present study explores the spatiotemporal variability of weather parameters in the Chittagong City Corporation (CCC) areas in Chittagong, Bangladesh. The current research was initially focused on understanding the dominant weather parameter changes (such as rainfall, air temperature, and relative humidity) from 1990 to 2020 weather data using geographic information system (GIS) and statistical analysis. The GIS map was prepared in four seasons (i.e., MAM, JJA, SON, and DJF) using Bangladesh Meteorological Department (BMD) data which considered the Co-Kriging interpolation technique in ArcGIS 10.8 software. An equal interval break classification with five (5) classes method was employed to classify each image. Further, the annual trend analysis was performed using the Mann-Kendall trend including Sen's slope estimator statistical analyses to support the present study. The study result reveals that the rainfall of CCC areas decreased in JJA among all seasons by 165.8mm in 2020 compared to 1990, whereas the annual trend of average rainfall also suggested the same. In CCC, overall, the seasonal air temperature in JJA from 1990 to 2020 rose by 3.3°C. In contrast, the data on relative humidity in JJA also observed an increasing trend (33.6%) during the same period. Meanwhile, the mean annual air temperature scenario has risen 1.1°C, and relative humidity decreased by 1.5% from 1990 to 2020. The outcome of this study will help researchers and city planners to understand the climate change thus helping to ensure the CCC becomes healthy, economically viable, resilient, and sustainable.

**Keywords:** Chittagong City Corporation (CCC), Kriging, Seasonal Variability, Mann-Kendall Trend Analysis, Weather Parameters.

#### **Cited As:**

Nath, B., Alam, S. M. A., Ahmmed Ripon, M. S. & Akter, N. (2024). Spatiotemporal variability analysis of weather parameters in Chittagong City Corporation, Bangladesh from 1990 to 2020, Advances in Geomatics, 2(2), 1-25. https://doi.org/10.5281/zenodo.14555114

<sup>&</sup>lt;sup>1</sup> Lab of Geoinformatics and Earth Observation Research (LGEOR), Department of Geography and Environmental Studies, Faculty of Biological Sciences, University of Chittagong, Chittagong 4331, Bangladesh.

<sup>\*</sup> Corresponding Author: B. Nath, 🖂 nath.gis79@cu.ac.bd 🕩 0000-0002-7598-0969

### INTRODUCTION

Climate change phenomena have been reported by many studies in the recent past, which is at present accelerating in a new dimension with different kinds of urban-related problems triggered by climate-induced hazards at the global and regional scales (Lambert et al., 2003; Dore, 2005). In this aspect, Bangladesh is directly affected by hydrological disasters (Kayano and Sansigolo, 2009). The geographical location of Bangladesh is characterized by distinctive environmental conditions which are observed climate change-induced impact at different scales. The naturally occurring phenomenon and their seasonal, and annual variations can be best determined with the help of multi-parameters of weather. Therefore, consideration of multiple parameters (e.g., rainfall, air temperature, and relative humidity) from the Bangladesh Meteorological Department (BMD) (BMD, 2021) is necessary to evaluate the difference and alteration of weather status over a specific period.

A long-term trend (Chattopadhyay et al., 2016) including seasonal and annual trend (Gümüş, et al., 2017) analyses of precipitation and the air temperature across the globe, especially in tropical urban areas (Ghumman and Horney, 2016; Asamoah and Ansah-Mensah, 2020) were considered to monitor weather pattern changes. Due to the rapid increase in population in the global city areas, exposure to extreme heat events will increase significantly (Meehl and Tebaldi, 2004; Jones et al., 2015). As a result, seasonal warming variation may raise the hottest temperature compared to the annual mean temperature (Kodra et al., 2014; Argüeso et al., 2016). With the pace of mean global temperature increase, it is expected that relative humidity level will also increase (Willett et al., 2007). Along with the increasing tendency of global temperature, precipitation pattern change was also observed due to the impact of global warming (Mishra, 2019; Falga and Wang, 2022). However, the scenario in Bangladesh reflected different levels of climatic data variability along with annual, seasonal, and monthly trends (Sunny et al., 2020). For example, in the past, the monsoon rainfall patterns, and their trends (Rahman et al., 1997) including the relationship study between rainfall and temperature change were analyzed for different regions of Bangladesh (Shahid, 2010).

Chittagong is a coastal and commercial capital city located in the southeastern part of Bangladesh that bears and shares great responsibilities in the country's economic progress. Therefore, introducing green infrastructure in response to climate change is necessary to foster sustainable growth and regional improvement (Gill et al., 2007; Norton et al., 2015). The weather condition of an area holds greater importance as it emphasizes seasonal and annual information of different weather parameters such as rainfall, air temperature, and relative humidity. Roy et al. (2015) focuses on the trend analysis of climate change in the Chittagong station in Bangladesh from 1979-2008 and observed an increasing trend of average rainfall, thus indicate a positive linear relationship between rainfall and time. In their specific study, the mean coefficient of variation (CV) of average annual humidity for Chittagong was observed at 78.0%.



The area under Chittagong City Corporation (CCC) has a provision to become a leading and healthy city for being in close contact with the Bay of Bengal (BoB) with port facilities. In recent times, it observed many weather-related disasters. For this reason, it is imperative to understand the changing weather conditions in this specific area as well as to know how the climatic parameters of CCC have changed gradually in recent times. In this connection, we have found very few literatures in this area which focuses on the multiple weather parameter changes. Hereby, only a recent study has been focusing on a single weather parameter knowing its changes at a spatiotemporal scale (Hossain, 2001). Therefore, understanding weather patterns through investigating of multiple parameter changes at a spatiotemporal scale over the CCC area is necessary for the city dwellers and city planners to adapt to the changing climate.

To understand the weather-changing conditions in CCC areas and to fill the existing research gaps, it is essential to use appropriate tools and techniques of the geographic information system (GIS) for spatio-temporal analysis of considering multiple weather parameters. Therefore, the present study aimed with the research questions, to know how the CCC area's multiple weather parameters have changed over time from 1990 to 2020, and how it varies according to different seasons, and annually, and at what trends suggests for these parameters. The main specific objectives of this study were: (a) to process the multiple weather parameters (i.e., rainfall, air temperature, and relative humidity) from the BMD weather datasets, (b) to prepare GIS maps based on the multiple weather parameters focusing on four seasons of each selective year at ten-year interval; and (c) to know the spatiotemporal variability analysis of multiple weather parameters from 1990 to 2020 in seasonal, and annual basis as well as its time series trends and magnitude of change using Mann-Kendall trend and Theil Sen's slope estimator test. The present investigation result will help urban decision-makers and planners to know the CCC's changing weather parameters by targeting sustainability development goals (SDGs) no.-11, to maintain the city healthy, economically viable, resilient, and sustainable.

#### 1. MATERIALS AND METHODS

### 1.1. Study area

The study area is situated between 22°14′-22°24′ N latitudes and 91°46′-91°53′ E longitudes as shown in Figure 1. It is bounded by Anowara Upazila in the south, Sitakunda in the North, and Boalkhali in the east with distinctive topography which characterized into two types such as 'lowland hills' and 'undulating lowlands' (Islam et al., 2024). The elevation of the CCC varies significantly from 7 m to 79 m above sea level (Chittagong Division Topographic Map, 2024; Islam et al., 2024). The geological distribution of CCC is divided into two deposits such as tertiary hill deposits aligned with NW-SE direction with the surrounding quaternary slopes and valley deposits in the west and fluvial-tidal deposits in the NE, E, and SE directions.

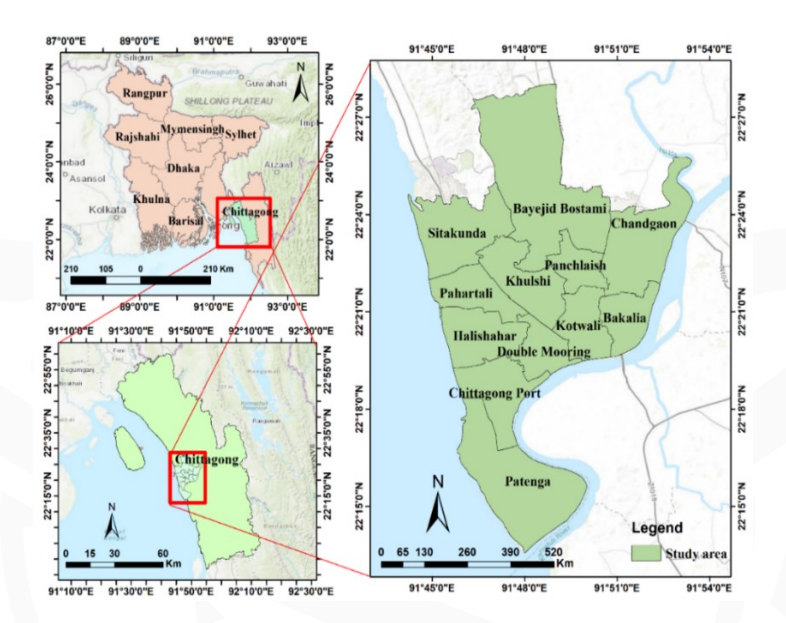


**Figure 1.** Location of the study area (CCC). In the top left, the Chittagong district is shown over the Bangladesh district map, in the bottom left, CCC overlays on the Chittagong district, and in the right panel, CCC is represented with 12 Thana's boundaries. In each panel, base imagery is displayed from the ESRI world base map.

The Bay of Bengal (BoB) is closely attached to the west side of the CCC area. The urban growth trend of the CCC area is observed in the NE direction, and on the southern side, where its boundary limits due to the presence of the Patenga Sea Beach. The annual average rainfall, air temperature, and relative humidity of CCC in 2021 are 220 mm, 25.8°C, and 77.7%, respectively (BMD, 2021). Patenga is the nearest meteorological station of CCC that considered in this study. The tropical monsoon climate system prevails in Patenga (Kottek et al., 2006). The district yearly temperature mentioned above is -1.9% lower than Bangladesh's averages and Patenga typically has 151.5 rainy days annually.

In the study area, during the year 2020, eight distinct land use and cover (LULC) groups are identified by Islam et al., (2024) which shared as agricultural land (11.5%) fallow land (9.66%), trees outside of forest (TOF) (26.2%), hill vegetation (6.08%), built-up (34.6%), mangrove (0.4%), pond/lake (2.9%), and river (8.7%). The study area's LULC has undergone changes in the period from 1990 to 2020 as observed through satellite images, which are increasing in built-up (278.5%), pond/lake (407.7%), river (10.1%) and declining trends observed in agricultural land (61.6%), hill vegetation (43.3%), mangrove forest (30.7%), fallow (22.0%), and TOF land (8.8%) (Islam et al., 2024).

### 1.2. Data

The data used in this study from 1990 March to 2020 February were collected from the Bangladesh Meteorological Department (BMD) (BMD, 2021) as daily rainfall, air temperature, and relative humidity. At the initial stage, the daily data supplied by the BMD for all three parameters were converted into

monthly data, then monthly to annual which performed within the MS Excel environment.

Based on the collected data, a shapefile was created within the ArcGIS 10.8 software by considering all 34 ground weather meteorological stations and corresponding datasets. In our case, the name of the nearest meteorological station is Patenga which is close to the CCC boundary. The location of meteorological weather stations are overlaid with the Bangladesh district-level boundary is shown in Figure 2.

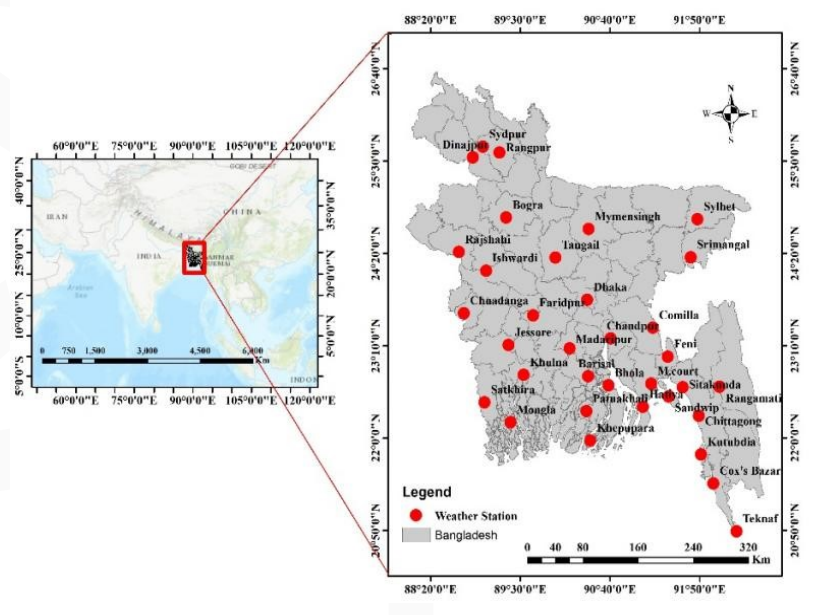


**Figure 2.** The location of meteorological weather stations in Bangladesh is considered for interpolating selected multi-parameters of the meteorological datasets.

### 1.3 Methodology

The study has adopted multiple steps to complete the data analysis, map classification, and representation are presented in the flowchart of the methodology as shown in Figure 3. The detailed methodological breakdown is given in the following sub-section from 1.3.1 to 1.3.2.

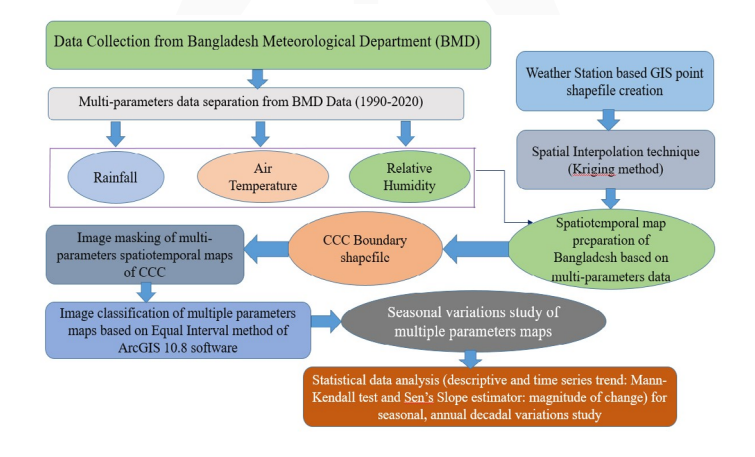
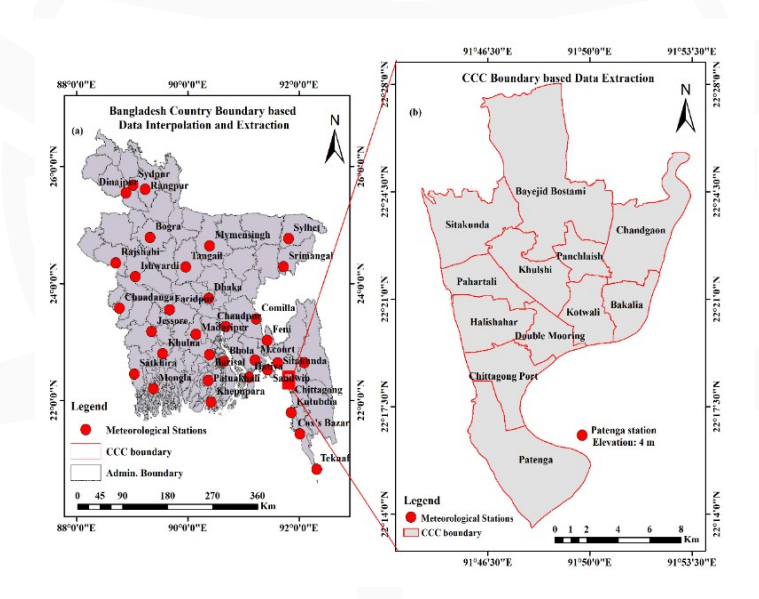


Figure 3. Flowchart of the methodology used in this study

### 1.3.1 Spatial interpolation techniques and GIS map preparation method

In this study, 34 ground station-based data were used for spatial interpolation after data separation. It is the process of using points with known values to estimate values at other unknown points. The spatial interpolation technique can calculate specific values at locations without recorded data using readings of known values at nearby weather stations. The spatiotemporal maps were created following the Geostatistical Co-Kriging method in ArcGIS 10.8 software using each parameter separated from the combined datasets (Figure 4).



**Figure 4.** Data interpolation and extraction techniques were performed based on 34 meteorological stations by adopting Bangladesh country boundary and masking operations done based on the CCC study area boundary.

In this aspect, Bangladesh's administrative boundary shapefile was used to mask each spatial map (Figure 4a). The Co-kriging is a technique considered for the overall visualization of time-series datasets. For the convenience of work, all three categories (i.e., rainfall, air temperature, and relative humidity) based maps have been prepared at 5-range class intervals following the equal interval classification method to know its spatial variability, which is used for final level image masking considering the CCC boundary (Figure 4b).

By following the above method, a series of maps have been created for the rainfall, air temperature, and relative humidity data of the study area based on once every ten years such as 1990, 2000, 2010, and 2020. Further, the specific year was divided into four distinct seasons such as March-April-May (MAM), June-July-August (JJA), September-October-November (SON), and December-January-February (DJF). In this study, the seasons are represented in the corresponding text and mapping as MAM, JJA, SON, and DJF. To give the classification image a more prominent look, three color ramps were selected for the three different parameters such as red to blue color ramp for rainfall distribu-



tion, green to red color ramp for air temperature, and yellowish gray to blue for relative humidity distribution.

### 1.3.2 Descriptive statistical data and Time series trend analysis method

In the climate change study, a minimum of 25-30 years of long-duration climatic data is required to ensure the statistical validity of the trend results (Burn and Elnur, 2002; Kahya and Kalayci, 2004). In this stage, the present study intends to explore the weather conditions of the CCC areas from past to present (1990-2020) and this has been done with the aid of MS Excel to calculate descriptive statistics such as minimum, maximum, mean, standard deviation of the seasonal, and annual basis. Moreover, during data processing, different steps were followed, i.e., first, the multiple weather parameters data from the BMD (BMD, 2021) were accumulated and rearranged in an orderly manner based on selected years.

Second, this temporal data has been used for time series and trend analysis by using the Mann-Kendall trend (Mann, 1945; Kendall, 1975) and Sen's slope estimator (Sen, 1968) tests of XLSTAT 2024.2.2.1422 version, which worked as a plugin with MS Excel software. In general, to detect monotonic trends from a series of environmental, climatic, and hydrological data, non-parametric Mann-Kendal trends and Sen's slope estimator tests were considered widely by the researchers due to their advantages in time series data over other tests (Deka et al., 2019; Aditya et al., 2021; Nyembo et al., 2021; Frimpong et al., 2022; Kawser et al., 2022; Sudarsan and Lasitha, 2023). The non-parametric Mann-Kendall test typically detected an upward and downward trend, and in test interpretation, the meaning of H0 is: there is no trend in the series, and Ha is: there is a trend in the series, and, the decision could be made in the following way, if the computed p-value is greater than the significance level alpha=0.05, one cannot reject the null hypothesis H0, and vice versa. On the other hand, Sen's slope estimator test calculated the slope of the data (linear rate of change), and intercept (Sen, 1968).

In this study, to test the Mann-Kendal trend and Sen's slope, the significance level is 5% (alpha 0.05), an approximation has been used to compute the p-value (two-tailed) and the Confidence Interval (CI) % (Sen's slope) is 99.

### 2. RESULTS

In the present study, different selective time-oriented maps of rainfall, air temperature, and relative humidity are analyzed and presented systematically in the following sections. The study reveals that the CCC areas have observed changes in different weather parameters based on the data from 1990 to 2020.

## 2.1 Spatio-temporal variability analysis of multiple weather parameters in CCC (seasonal scenario)

### 2.1.1 Observed seasonal rainfall variability in CCC areas from 1990 to 2020

Figures 5(a-p) represent the variability of rainfall distribution in CCC at ten-year interval variation such as March 1990 to February 1991, March 2000 to February 2001, March 2010 to February 2011, and March 2019 to February 2020. The seasonal rainfall distribution of CCC from MAM 1990 is shown in Figure 5a. NE of Chandgaon, and Baizid Bostami areas observed the maximum rainfall from 168.1-172.8mm range (Figure 5a) and moderate rainfall 158.6-163.3mm recorded at Chandgaon, Bakalia, Kotwali, NE Pahartoli and Sitakunda areas. The lowest rainfall was 225.7-233.1mm experienced in Patenga, Double Mooring, Kotowali, Bakalia, and part of Chandgaon (Figure 5a).

However, during JJA (Figure 5b) the same year, the CCC observed the highest 255.6-262.9mm rainfall at Baizid Bostami and part of Chandgaon areas. Compared to this, the northern, central, and southern parts of CCC, especially, Patenga, Chittagong Port, Double Mooring, and a small part of Chandgaon and Panchlaish practically received the lowest rainfall (225.7-233.1mm). The seasonal rain in SON during 1990 with the maximum rainfall from 99.1mm to 101.1mm occurred at part of Chandgaon, and NE of Baizid Bostami (Figure 5c). Medium rainfall occurred as 94.3-96.6mm at Bakolia, Panchalish, Khulsi, part of Chandgaon, and Baizid Bostamiand (Figure 5c). On the other hand, in southern and south-western parts of the Patenga and west of Chittagong port city and Halishar experienced the lowest rainfall (89.4-91.8mm) in this specific season. However, in DJF (the coolest period), this area received 10.9-11.4mm of rainfall in maximum parts of CCC, except NE of Chandgon, and Baizid Bostami which observed 11.9-12.3mm, and 12.9-13.2mm of rainfall (Figure 5d).

Figure 5e represents the highest rainfall (285.3-289.3mm) during MAM in 2000 in the eastern part of Bakalia, Chandgaon, and Panchlaish. On the other hand, the least rainfall (269.2-273.2mm) was observed in SW of Patenga and Halishahar (Figure 5e). This rainfall showed a different variation pattern from JJA in 2000, where the entire Patenga received the maximum rainfall (672.6-688.4mm) (Figure 5f). Compared to the Patenga, the eastern part of Panchlaish, Chandgaon, Bakalia and Double Mooring had practically observed 656.9-672.6mm of rainfall, considered as the 2nd highest. Moreover, Figure 5g shows minimum rainfall (174.8-177.6mm) from SON 2000 observed in north of Bayezid Bostami. During that time, the maximum rainfall (185.9-188.7mm) was received by Patenga, Chittagong port and part of Double Mooring and Halishahar areas (Figure 5g).

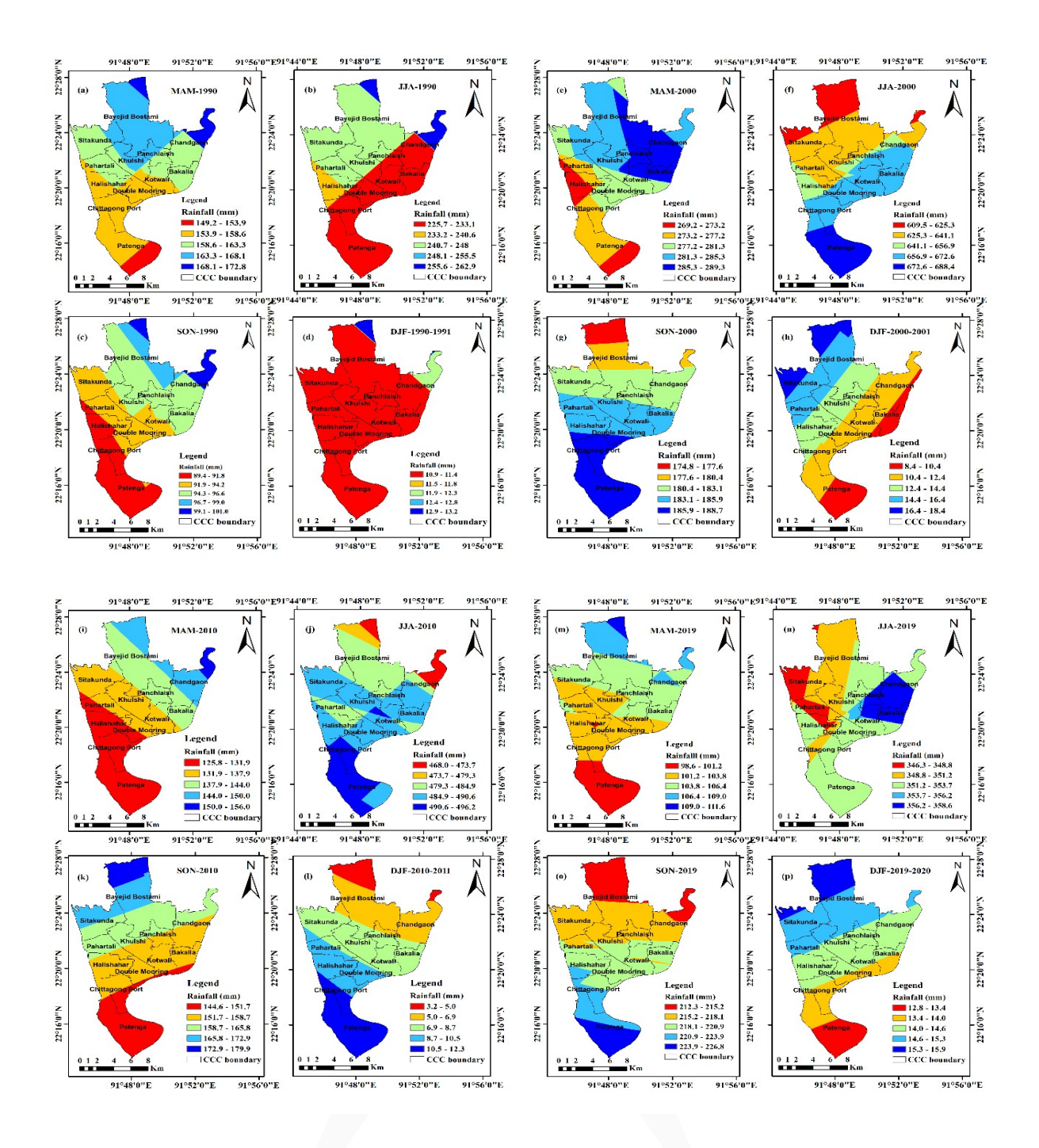


**Figure 5.** Rainfall distribution in CCC areas in seasonal basis for different periods (at 10 year interval) from March 1990 to February 1991, March 2000 to February 2001, March 2010 to February 2011, and March 2019 to February 2020; (a) MAM 1990 rainfall, (b) JJA 1990 rainfall, (c) SON 1990 rainfall, (d) DJF 1990-1991, rainfall, (e) MAM 2000 rainfall, (f) JJA 2000 rainfall, (g) SON 2000 rainfall, (h) DJF 2000-2001 rainfall, (i) MAM 2010 rainfall, (j) JJA 2010 rainfall, (k) SON 2010 rainfall, (l) DJF 2010-2011 rainfall, (m) MAM 2019 rainfall, (n) JJA 2019 rainfall, (o) SON 2019 rainfall, (p) DJF 2019-2020 rainfall distribution (Source: authors prepared maps based on BMD data).

Figure 5h represents the scenario of December 2000 to February 2001. During that time, the maximum (16.4-18.4mm) and minimum (8.4-10.4mm) rainfall were observed at SW of Baizid Bostami, and Sitakunda areas, and SE Patenga and Bakalia areas, respectively. Figure 5i represents the summer rainfall of the year 2010, where, the maximum amount of rainfall (150.0-156.0mm) took place only in NE of Chandgoan areas, and moderate rainfall was received in the Bakalia, Panchlaish and part of Baizid Bostami areas. However, the maximum amount of rainfall (490.6 to 496.2mm) was observed in SW of Patenga and Chittagong Port areas, and minimum (468.0-473.7mm) rainfall in the NE areas of Chandgaon during the rainy season (JJA) (Figure 5j). The remaining periods represent the rainfall scenario from SON and DJF from 2010 to 2011 time periods respectively (Figure 5k, and Figure 5l).

On the other hand, the recent scenario of 2019 shows a clear overview of rainfall variability in the CCC areas. The areas of Patenga, and a tiny part of Halishahar (red color) experienced the minimum rainfall of nearly 98.6-101.2mm, whereas, the areas marked with green color received moderate rainfall in the range of 103.8-106.4mm (Figure 5m). Figure 5(n–p), shows the rainfall distribution pattern from 2019 JJA, SON, and 2019 December to February 2020. During these three periods, the lowest rainfall (12.8-13.4mm) was recorded in the winter season at South of Patenga areas.

### 2.1.2 Observed seasonal air temperature variability in CCC areas from 1990 to 2020

In this study, based on four seasons in each selective year, temperature distribution maps are prepared for the years 1990, 2000, 2010, and 2020 (Figures 6a-p). In the year 1990, the maximum temperature in the summer season (MAM) was observed as 11.0°C-11.1°C at parts of Patenga, whereas, the minimum temperature in this season was observed at 10.6°C-10.7°C at Bayezid Bostami, Sitakunda, and some parts of Pahartali areas (Figure 6a).

Figure 6b represents the air temperature scenarios during the rainy season (from JJA 1990) observed at Patenga, Chittagong port, and the Double mooring area (Figure 6b). The maximum and the lowest air temperatures of the rainy season were observed at parts of Patenga at 12.3°C-12.4°C and 11.9°C-12.0°C, at major shares of Sitakunda, and NW part of Bayezid Bostami, respectively. On the other hand, from the spring season (SON), and winter season (DJF) (1990-1991), the maximum temperature was observed at 11.2°C-11.3°C (Figure 6c), and 9.0°C-9.1°C (Figure 6d), respectively.

However, during summer time (MAM) in 2000, the air temperature at different places in CCC areas was observed maximum of 13.6°C-14.2°C (highlighted in the red color at the NE part of Bayezid Bostami), and a minimum air temperature observed close to 10.4°C-11.2°C (represented by forest green color in SE of Patenga) (Figure 6e). Further, in 2000, the temperature increase was observed from 14.3°C to 15.0°C during JJA (Figure 6f), whereas, in the same year from SON, the maximum value was observed in a slightly decreased condition from 13.6°C to 14.3°C was observed in (Fig. 6g).

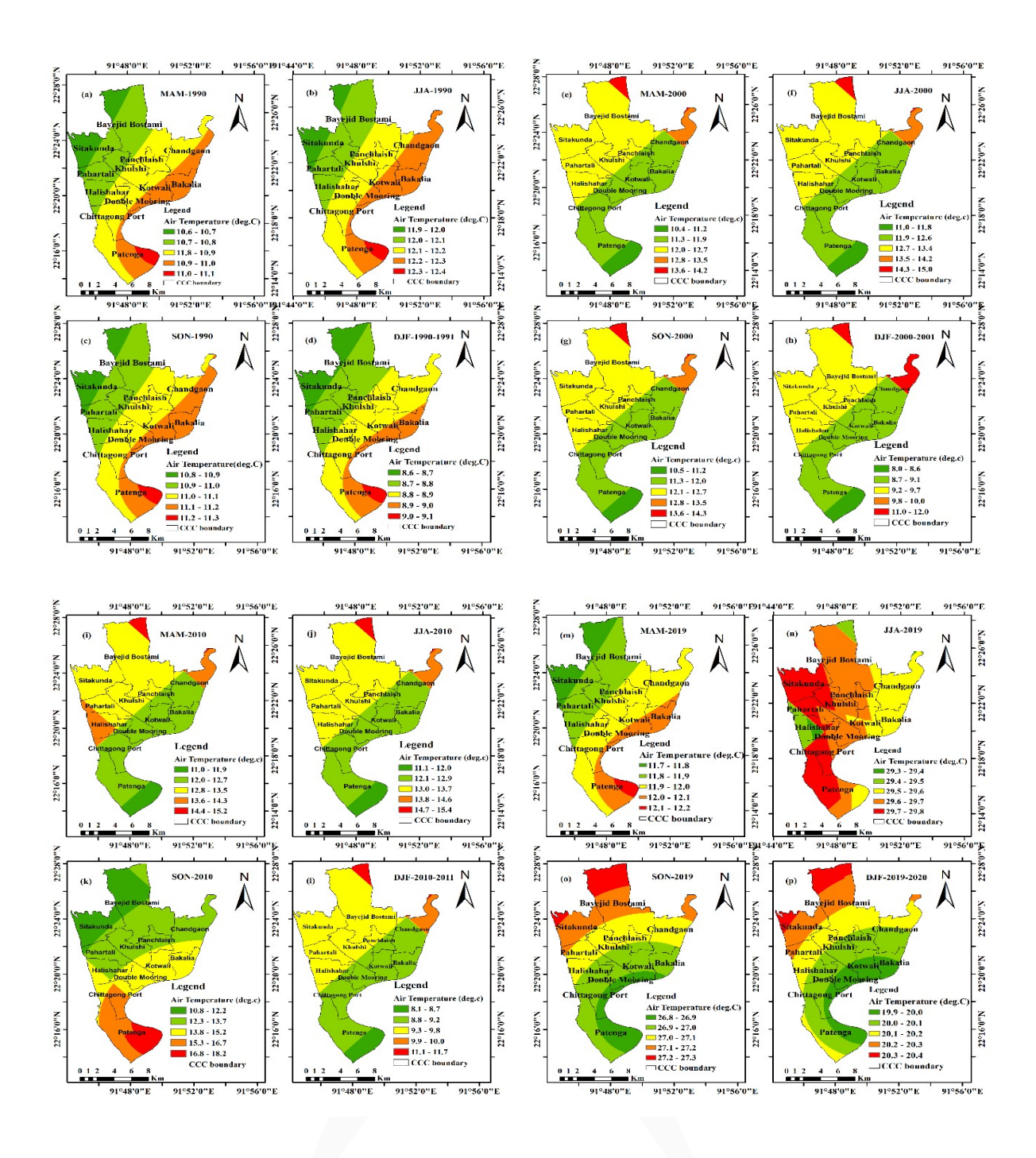


**Figure 6.** Air temperature distribution of CCC in seasonal basis for different periods from 1990 to 1991, 2000 to 2001, 2010 to 2011, and 2019 to 2020; (a) MAM1990 air temperature, (b) JJA 1990, (c) SON1990, (d) DJF 1990-1991 air temperature, (e) MAM 2000 air temperature, 2000 air temperature, (g) SON2000 air temperature, (h) DJF 2000-2001) air temperature distribution, (i) MAM 2010 air temperature, (j) JJA 2010, (k) SON 2010, (l) DJF 2010-2011 air temperature (m) MAM 2019 air temperature, (n) JJA 2019, air temperature (o) SON 2019 air temperature, (p) DJF 2019-2020) air temperature distribution (Source: Map prepared by authors based on BMD data).

Thereafter, from DJF (2000 to 2001), the maximum temperature was suddenly observed in a decreasing trend from 11.0°C to 12.0°C due to winter (Figure 6h). Figure 6i and Figure 6j represent the air temperature scenarios 2010 in the CCC areas for the two consecutive seasons i.e., MAM, and JJA, respectively. The maximum air temperature was observed from 14.4°C-15.2°C located at the NE part of Bayezid Bostami (Figure 6i), whereas, the lowest air temperature was recorded as 11.0°C-11.9°C at the south and SE part of Patenga areas (Figure 6j).

In comparison to the above, the air temperature scenario was observed differently in several places during spring (Figure 6k) and winter seasons from December 2010-February 2011 (Figure 6l). Moreover, in recent times, from MAM 2019, the lowest temperature of nearly 11.7°C-11.8°C was observed at NW of Bayezid Bostami and Sitakunda areas, and a maximum of 12.1°C-12.2°C was observed at eastern part of Patenga (Figure 6m). Eventually, the temperature showed in dramatic rising trend, and the maximum was observed between 29.7°C-29.8°C in several parts of the area, especially in the west of Patenga, SW of Double Mooring, the central area of Pahartali and the entire Sitakunda areas (Figure 6n), which had been slightly lower during SON 2019 (Figure 6o). However, during winter time (December 2019-February 2020), the air temperature was observed as a maximum between 20.3°C-20.4°C in the north, NW of Bayezid Bostami and a tiny NW part of Sitakunda area (Figure 6p).

### 2.1.3 Observed seasonal relative humidity variability in CCC areas from 1990 to 2020)

In Figure 7a, 33.4%-33.5% relative humidity was considered as maximum humidity marked as blue area in eastern part of Patenga, and the NW of Bayezid Bostami and Sitakunda were marked as the lowest relative humidity areas as 32.8%-32.9%. On the other hand, moderate relative humidity (33.1%-33.3%) was observed at Double Mooring, SE of Bayezid Bostami, entire Panchlaish, Khulsi, and parts of Halishahar, and major shares of Chittagong port areas. The highest relative humidity amounts to 43.2%-45.7% observed in NE of Bayezid Bostami shown in blue areas, whereas yellowish gray color marked as the least humidity close to 33.3% to 35.8% (Figure 7b).

Compared to the above, the wettest period (SON) in 1990 was found to have a maximum of 38.4% to 39.1% relative humidity in the NE of Bayezid Bostami which was unraveled as the absolute humidity (Figure 7c), and maximum shares of Patenga experienced 35.3%-36.1% as the lowest humidity. However, moderate humidity up to 36.8%-37.6% was observed in Khulsi, Kotwali, and NE of Sitakunda areas (Figure 7c), whereas, it was observed nearing 33.1%-33.3% (marked in blue color) in the NE of Patenga, Double Mooring and Bakalia areas (Figure 7d). In the next decade, during MAM 2000, the maximum relative humidity was observed at several places i.e., east Double Mooring, Bakalia, and some parts of Kotwali, Panchlaish, and Chandgoan areas (Figure 7e).

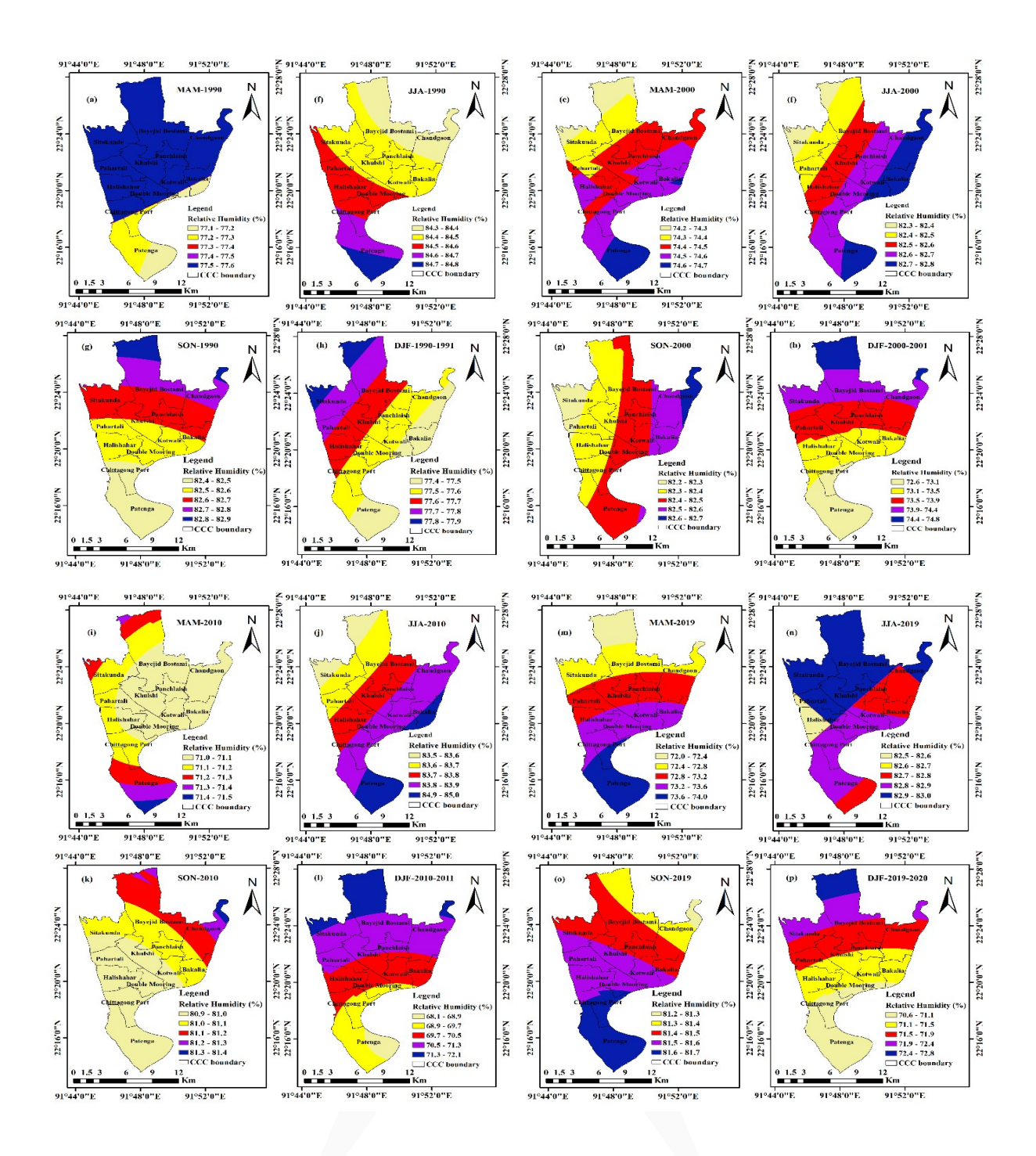


**Figure 7.** Seasonal relative humidity distribution of CCC in different periods from 1990 to 2020, 2000 to 2001, 2010 to 2011, and 2019 to 2020. (a) relative humidity of MAM 1990, (b) relative humidity of JJA 1990, (c) relative humidity of SON 1990, (d) relative humidity of DJF 1990-1991 (e) relative humidity of MAM 2000, (f) relative humidity of JJA 2000, (g) relative humidity of SON 2000, (h) relative humidity of DJF2000-2001, (i) relative humidity of MAM 2010y, (j) relative humidity of JJA 2010, (k) relative humidity of SON 2010, (l) relative humidity of DJF 2010-2011 (m) relative humidity of MAM 2019, (n) relative humidity of DJF 2019-2020.

On the other hand, moderate and lowest humidity were observed close to 31.8%-32.0% (red color), and 31.6%-31.7%, (yellowish gray color) in the north and NW of Sitakunda, and a small part of NW Bayezid Bostami, respectively (Figure 7e). From JJA in 2000, around 35.2%-35.4% relative humidity was observed in the highest form at the NE Patenga area, and the lowest 34.4%-34.6 % was at NW of Sitakunda and Bayezid Bostami areas (Figure 7f). The scenario was observed differently (moderate humidity with 34.8%-35.0%) in central CCC regions, especially at Panchlaish, Kulshi, and Chittagong port areas (Figure 7f).

Moreover, during SON in 2000, the highest relative humidity around 41.8%-43.8% was observed in NE areas of Bayezid Bostami, and the lowest (31.4%-34.7%) was observed in SE of Patenga areas (Figure 7g). From December 2000 to February 2001, the highest and lowest relative humidity was recorded in the eastern part of Patenga and SW of Bayezid Bostami, and Sitakunda areas about 30.9%-31.0%, and 30.5%-30.6%, respectively (Figure 7h).

On the other hand, in MAM 2010, the highest relative humidity (33.2%-33.5%) was experienced in eastern part of Chandgoan, Bakalia, and Patenga areas, and the minimum relative humidity (32.2%-32.5%) was noticed in west of Sitakunda (Figure 7i). Further, during JJA in 2010, the relative humidity observed an increasing trend at 35.8-35.9% (Figure 7j), and the lowest humidity from 35.1%-35.2% was reported in the rainy season (yellowish gray color). However, the maximum relatively humidity during SON was observed in eastern Patenga (Figure 7k). Following these, the relative humidity continued to increase from December 2010 to February 2011 (Figure 7l), the highest was recorded (35.7%-37.8%) at a small part of NE Bayezid Bostami, and moderate relative humidity (42.2%-48.5%) was observed in different parts of the CCC areas especially Bayezid Bostami, Sitakunda, Pahartali, Halisahar, and a tiny parts of Panchlaish areas. However, at this time, the lowest relative humidity was traced as 27.5%-29.6% at the south and SE of Patenga.

In recent times (from MAM 2019), the areas in *CCC* especially the eastern part of Chandgaon, Bakalia, and Patenga areas observed the highest relative humidity (33.2%-33.5%) (Figure 7m), which continued to increase during JJA in 2019 as maximum relative humidity recorded 35.8%-35.9% (Figure 7n). From SON 2019, the highest and lowest relative humidity was observed as 34.9%-35.1% and 34.2%-34.4%, respectively (Figure 7o). Moreover, in the winter period (December 2019 to February 2020), the maximum relative humidity was observed as 30.9%-31.1% in eastern parts of Chandgo-an, Bakalia, and Patenga, and on the other hand, the lowest (30.5%-30.6%) was observed at NW of Sitakunda areas (Figure 7p).

## 2.2 Statistical variability analysis of multiple weather parameters based on mean seasonal, and annual data from 1990 to 2020

2.2.1 Descriptive statistical change analysis of multiple weather parameters

In this stage, the study focuses on the descriptive statistical analyses to get the seasonal variability of numerous weather parameters i.e., rainfall, air temperature, and relative humidity over the CCC areas from March 1990 to February 2020 by calculating the seasonal mean (average of three months) and it's coefficient of variation (CV%) of each specific year (at 10 year interval). The descriptive statistical results of the three multiple weather parameters are sequentially presented in Figures 8(a-f).

During rainy seasons (JJA) and winter (DJF) in the period from 1990 to 2020 are analyzed at 10 year interval. In this regard, the highest and the lowest rainfall were observed as 591.7mm and 10.3mm in the years 2000-2001 and 2010-2011, respectively (Figure 8a). However, in MAM, the highest 195.3mm and lowest 95.7mm rainfall were recorded in 1990-1991 and 2019-2020, respectively (Figure 8a), On the contrary, in SON maximum 196.0mm and lowest 33.3mm rainfall were observed in between 2000-2001 and 2010-2011, respectively (Figure 8a).

Among all the seasonal rainfall variability from March 1990 to February 2020 (at 10 year interval), the maximum 15.13% of CV was observed in DJF during 2000-2001 period (Figure 8b). On the other hand, the lowest rainfall variability (CV 0.59%) was noticed in MAM during the same period (Figure 8b). Meanwhile, in JJA of the 2019-2020 period, the maximum air temperature peaked at 29.6°C, and the minimum observed in DJF at 19.9°C during the 2000-2001 period (Figure 8c). The maximum CV% of air temperature variability was observed at 14.25% in SON during the 2010-2011 period and the lowest variability was observed in JJA at 0.07% during the 2019-2020 period (Figure 8d).

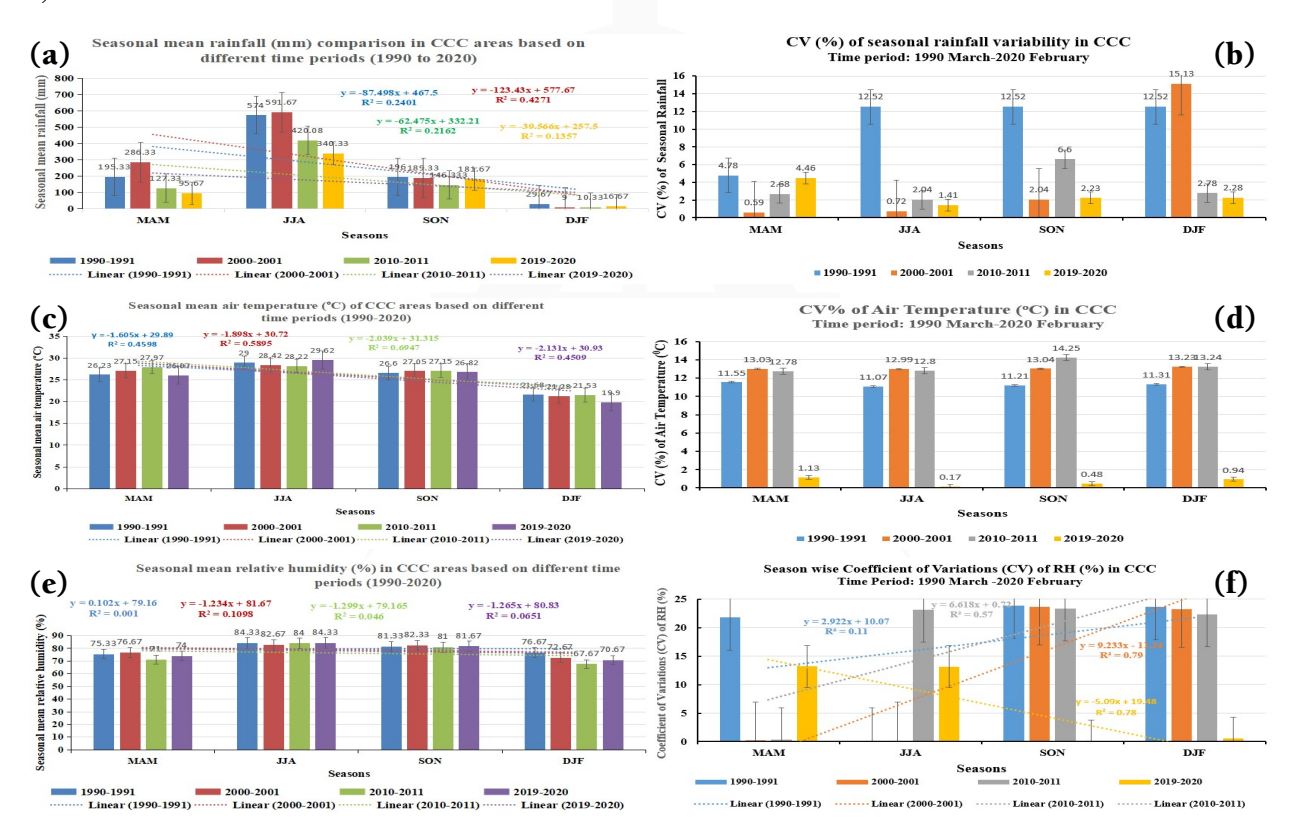


**Figure 8.** Time-series data analysis of the seasonal rainfall, air temperature, and relative humidity and its co-efficient of variation (CV%) from 1990 to 2020 (at 10 year interval), (a) seasonal mean rainfall observed from 1990 to 2020 (at 10 year interval); (b) CV% of seasonal rainfall variability from 1990 to 2020 (at 10 year interval) (c) seasonal air temperature observed from 1990 to 2020 (at 10 year interval); (d) CV% of air temperature from 1990 to 2020 (at 10 year interval); (e) seasonal relative humidity observed from 1990 to 2020 (at 10 year interval), and (f) season wise coefficient of variation (CV%) of relative humidity from 1990-2020 period (at 10 year interval).

On the other hand, the mean relative humidity was observed highest and lowest at 84.3% in 1990 JJA and 66.7% in DJF during 2019-2020 (at 10 year interval), respectively (Figure 8e). The season-wise CV variation of relative humidity was observed at maximum (24%) in SON during the 1990-1991 period, and the lowest variation near 0% was observed in SON during the 2019-2020 period (Figure 8f). The negative trend with R² value of 0.78 in CV indicates a downward trend in recent times (2019-2020) compared to the past (1990-1991). However, during MAM the CV% variation of relative humidity shows a positive trend with R² value of 0.11. This trend was positive also during the 2010-2011 period with R² value of 0.57, as well as during the 2000-2001 period. The relative humidity variability was also observed in a positive trend with R² value of 0.79 (Figure 8f).

## 2.2.2 Seasonal variability analysis of multiple weather parameters based on Mann-Kendall and Sen's Slope estimator trend tests

The Mann-Kendall and Sen's Slope estimator trend tests generally gives us the trends in the time series data with the statistical significance results (Frimpong et al., 2022). In this test, Figures 9(a-l) detects the seasonal variability trends in multiple weather parameters based on the period 1990-2020. In the case of mean seasonal rainfall trend, MAM (Figure 9a) and DJF (Figure 9d) seasons show a downward trend of rainfall in the time series data, whereas JJA (Figure 9b) and SON (Figure 9c) show an upward trend of rainfall, and in JJA season, extreme rainfall increases observed in 2015. This upward and downward trend was detected at a confidence level of 95% (5% significance level), and Sen's slope test shows that the highest and lowest mean seasonal rainfall value was observed at 950mm, and no rainfall in the JJA and DJF seasons. Among all the seasonal rainfall trend graphs, the p values are observed higher (p > 0.05) which have no significant trend in the data series except in the season of DJF (p < 0.05), which has a slope value (-0.4848) indicate a negative trend (y = -0.4848x + 982.05) (Figure 9d).

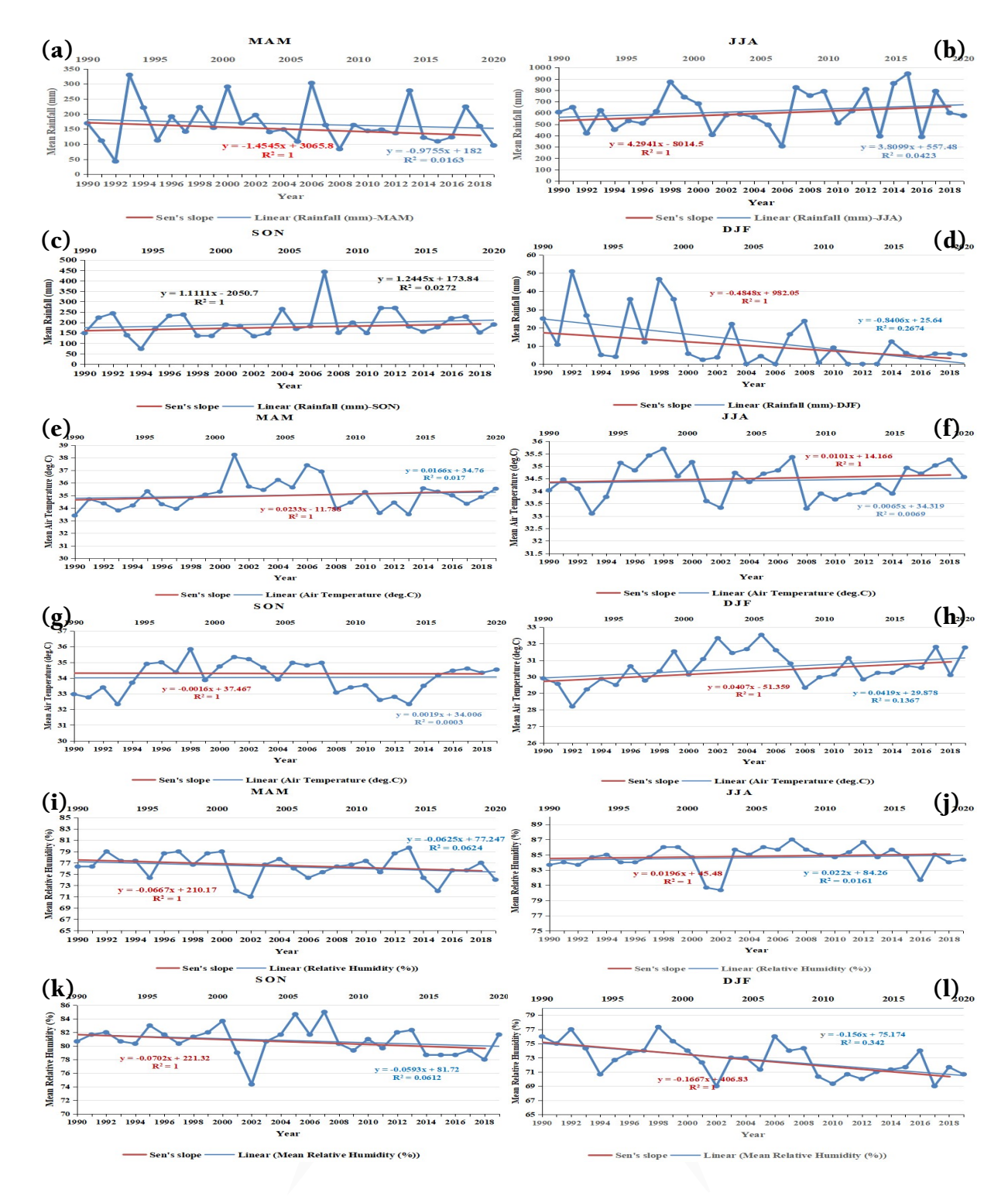


**Figure 9.** Seasonal mean weather parameters changes in CCC areas for the time period from 1990-2020; (a) seasonal mean rainfall (mm) trend for MAM, (b) same but for JJA, (c) same but for SON, (d) same but for DJF, (e) seasonal mean air temperature (°C) trend for MAM, (f) same but for JJA, (g) same but for SON, (h) same but for DJF, (i) seasonal mean relative humidity (%) trend for MAM, (j) same but for JJA, (k) same but for SON, (l) same but for DJF of CCC areas during 1990-2020 time periods.

However, the results for the Mann-Kendall and Sen's Slope estimator trend tests for seasonal air temperature over the period 1990-2020 are presented in Figures 9e-h. Among all mean seasonal air temperature ( $^{\circ}$ C) graphs, it has been observed the higher p values (p > 0.05) in three different seasons such as MAM, JJA, SON (Figures 9e-g) except in the season DJF (Figure 9h), which has the lower p values (0.027) (p < 0.05), and observed significant trend in the data series with the slope value (0.0407) indicate a positive trend of y = 0.0407x - 51.359 (Figure 9h).

Moreover, considering the similar time period, the results of the trends for mean seasonal relative humidity (%) (Figures 9i-l) also suggests the higher p values (p > 0.05) for the MAM, JJA, SON (Figures 9i-k) except for the season DJF (Figure 9l), which has the lower p values (0.003) (p < 0.05), and observed significant trend in the data series with the slope value (-0.1667) indicate a negative trend of y = -0.1667x + 406.83 (Figure 9l).

### 2.2.3 Annual variability analysis of multiple weather parameters based on Mann-Kendall and Sen's Slope estimator trend tests

In the case of annual rainfall variability in CCC areas over the period from 1990 to 2020 (Figures 10a-c), the mean maximum and minimum rainfalls were observed at 362.00mm and 188mm in 2007 and 1994, respectively. The obtained value of  $R^2 = 1$  expresses the acceptability of the rainfall trend as very strongly high with a non-significant increasing trend (p > 0.05), and then the p-value is observed at 0.015 (two-tailed) which indicates there is no variability exists in the data. The slope of the annual rainfall trend analysis suggests the rainfall will continue increasing and the positive slope value (0.9881) indicates a positive trend (y = 0.9881x - 1730.8) (Figure 10a).

However, in the air temperature annual variability analysis in CCC areas considering the same period, we observed a mean air temperature of  $34.6^{\circ}$ C in 2006, and a minimum air temperature of  $32.0^{\circ}$ C observed in 1993. In connection to this, the trend line of the annual air temperature from 1990 to Feb 2020, suggests a positive non-significant increasing trend (p > 0.05), and then the p-value is observed at 0.225 (two-tailed) indicates no variability in the existing data. The slope of the annual air temperature trend suggests it will continue to increase and the positive slope value (0.0233) indicates a positive trend (y = 0.0233x - 13.232) (Figure 10b).

On the other hand, the annual mean relative humidity varied significantly during the same period, where the maximum and minimum average relative humidity was observed at 80.5% and 72.8% in 1992 and 1991, respectively. Moreover, the overall annual trend line shows a decreasing pattern with a non-significant negative trend (p > 0.05), and then the p-value is observed at 0.068 (two-tailed) indicating no variability in the existing data series. The slope of the annual relative humidity trend suggests it will continue to decrease and the negative slope value (-0.0542) indicates a negative trend (y = -0.0542x + 186.96) (Figure 10c).

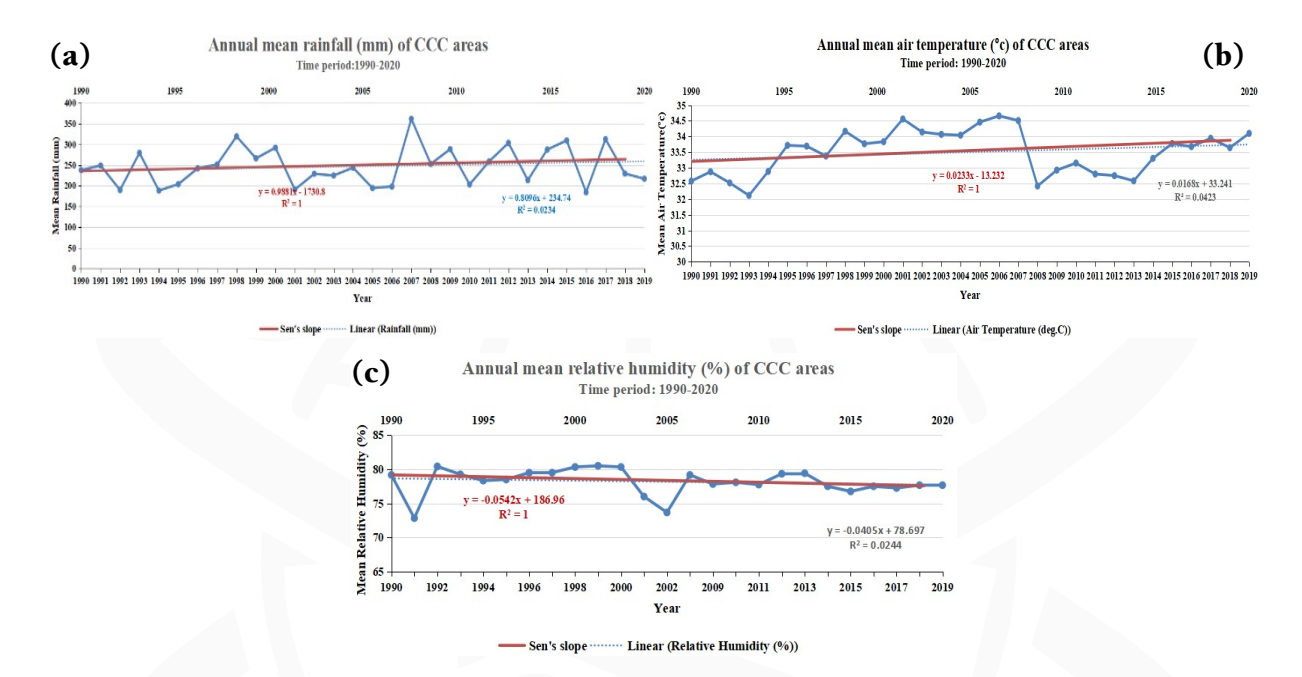


**Figure 10.** Annual mean weather parameters changes in CCC areas; (a) annual mean rainfall (mm), (b) annual mean air temperature (°C), and (c) annual mean relative humidity (%) trends of CCC areas during 1990-2020 time periods (Source: base data collection from BMD, 2021 and data analyzed and graphs prepared by authors using Mann-Kendall Trend test and Sen Slopes estimator with XLSTAT add-in software.

### 3. DISCUSSION

Climate variables inside the urban area are influenced by the interaction between urban elements and the prevailing weather conditions such as air temperature, relative humidity, wind speed, solar radiation, and rainfall. The different micro-climatic variable's effect on the local environment is found in the pieces of literature, but not sufficient for a city like CCC. Numerous urban city areas have reported increases in sudden rainfall due to increases in urbanization (Pathirana et al., 2014), which can lead to flood hazards in the city areas (Umer et al., 2023). Moreover, Cong and Brady (2012) reported a negative correlation between air temperature and rainfall.

However, as far as our concern and existing literature gaps suggest that no such weather parameters are seemingly integrated with a single area's investigation especially focusing on the micro-climatic urban context in Chittagong. In this context, cities like CCC are focused on better understanding its changing weather conditions that have already impacted and necessary to find out, when and where the weather parameters have changed in the CCC areas. Therefore, to monitor the weather changing phenomena in CCC areas, better spatial interpolation technique is needed, and in this study, we have considered ordinary kriging interpolation with exponential model which was adopted by Tong et al., (2015), as it can provide better interpolation accuracy with less mean error.

In general, human health is directly influenced by the increase in air temperature and relative humidity due to the urban heat island (UHI) effect (Zhao et al., 2014). The mean surface air temperature changes in all seasons were observed to increase over the entire India, along with long-spell rainfall events showing a decreasing trend in monsoon season in the last 54 years of meteorological data (Dash et al., 2006). The study conducted by Pamarthi, (2020), confirmed temperatures are warming in all major cities of India, and the annual average temperature in Hyderabad city is 26.0°C. In the winter season, the air temperature is low (22.5°C), and high (31.0°C) during the pre-monsoon season, Moreover, Roy et al. (2015) observed an average relative humidity for Chittagong was 78.0%, including the trend of average rainfall increasing as well as identified positive linear relationship between rainfall and time. Further, Khan et al., (2019) performed a change study in Bangladesh from 1988 to 2017 and they confirmed that the average monthly Tmax and Tmin have increased significantly which supporting our study results.

The divergence between mean and extreme air temperature changes also aligns with many previous studies (Ballester et al., 2010; Kodra et al., 2011; Argüeso et al., 2016). Moreover, a study focused on the impact of rainfall on air temperature, relative humidity, and thermal comfort, and observed that rainfall affects in different ways in the urban impervious areas (Acero et al., 2024). Therefore, it is established that the relation between relative humidity and air temperature is inversely proportional. If the temperature increases, it will reduce relative humidity, and thus the air will become drier.

### **CONCLUSION AND THE WAY FORWARD**

The spatiotemporal variability analysis of weather parameters over the *CCC* areas set an example for the regular phenomena that occur in a distinctive region. The worldwide changes in weather indices bring out information about the atmospheric conditions which supports the weather forecast, crop production, and estimated agricultural water balance. But the scenario is different in Bangladesh which has an inconsiderable number of research on this subject. This is also an important step toward geospatial research in Bangladesh especially to observe the recent past (from March 1990 to February 2020) changes and trends in the important climatic parameters over the *CCC* regions done by the combination of geospatial and statistical techniques. The multiple weather parameters mainly rainfall, air temperature, and relative humidity are subject to change due to physiographic, and socio-economic conditions. This alteration would be the reason for a change in climatic conditions in the study area especially it reflects in the yearly average air temperature which increased by 1.1°C.

However, in season-based analysis, the MAM season observed the highest temperature, the rainy season confronts the highest rainfall and winter faces the lowest temperature of the year. The highest humidity was detected during the JJA whereas the lowest was observed between the MAM and DJF. The spatial distribution of multi-parameters-based mapping exercises were performed with the aid of ArcGIS 10.8 software based on the BMD data. In this aspect, the equal interval classification method

(five classes) was considered during ordinary kriging interpolation process.

The outcome of this study shows that the south-western Patenga and Chittagong port areas are confront with the BoB which has given the advantages of geographic locations and accepted 73.7% of relative humidity. On the other hand, Sitakunda, Baijid Bostami, Pahartoli and Khulshi accepted 360.02mm of rainfall because of the presence of northern hilly area. Sitakunda and Baizid Bostami received the maximum rainfall in JJA. The sea-sided areas like Patenga and Chittagong port assent the lowest rainfall where the maximum air temperature was observed. The areas like Patenga, Chittagong Port, and the south side of Double Mooring are those places that experience the highest air temperature. In contrast to these parameters, the CCC area experiences the utmost relative humidity in the rainy season which occurs between JJA. The most relative humidity experienced areas are close to the river bank located at the Double Mooring, coastal-sided Chittagong port, and Patenga areas.

Finally, the knowledge of this spatial disparity will help to understand the changing nature of weather parameters in the past and recent times that helps to manage UHI effects, agriculture and crop production in the CCC areas. The outcome of this study may first help meteorologists to make quick decisions for possible forecasting in the CCC areas, and second, the trend values of multiple parameters will assist city planners and administrators in preparing and tackling the upcoming weather conditions of CCC. Moreover, making proper decisions based on the continuous monitoring of the weather conditions helps to achieve the particular sustainable development goal (SDG No. 11), and as a result, the city will become healthy, economically viable, resilient, and sustainable.

**Acknowledgments:** The authors express their gratitude to the Bangladesh Meteorological Department (BMD) for providing us with the required datasets that used in this research. Moreover, the authors are highly grateful to the editor and two anonymous reviewers for their constructive comments and suggestions that helped us to improve our manuscript in its current form.

**Conflicts of Interest:** The authors of this paper declare no conflict of interest.

**Author's contribution:** All the authors of this paper have significantly contributed to the design of this research. 1st, 2nd, and 4th authors have drafted the manuscript and contributed equally. The 3rd author highly contributed to mapping and statistical analyses. Finally, 1st and 4th authors contributed to the manuscript in early-stage and post-submission review, editing, and mapping exercises. All authors finally agreed and approved the changes made in the revised version of the manuscript.

#### REFERENCES

Acero, J. A., Kestel, P. C., Dang, H. T. & Norford, L. K. (2024). Impact of rainfall on air temperature, humidity and thermal comfort in tropical urban parks. Urban Climate. 56, 1–16. https://doi.org/10.1016/j.uclim.2024.102051

- Aditya, F., Gusmayanti, E., & Sudrajat, J. (2021). Rainfall trend analysis using Mann-Kendall and Sen's slope estimator test in West Kalimantan. 2nd International Conference on Tropical Meteorology and Atmospheric Sciences IOP Conf. Series: Earth and Environmental Science 893 (2021) 012006. IOP Publishing. doi:10.1088/1755-1315/893/1/012006
- Argüeso, D., Di Luca, A., Perkins-Kirkpatrick, S. E., & Evans, J. P. (2016). Seasonal mean temperature changes control future heat waves. Geophysical Research Letters, 43, 7653–7660. https://doi.org/10.1002/2016GL069408
- Asamoah, Y., & Ansah-mensah, K. (2020). Temporal description of annual temperature and rainfall in the Bawku Area of Ghana. Advances in Meteorology, 2020(3402178), 1–18. https://doi.org/10.1155/2020/3402178
- Ballester, J., Radó, X., & Giorgi, F. (2010). Future changes in central Europe heat waves expected to mostly follow summer mean warming. Climate dynamics, 35, 1191–1205. https://doi.org/10.1007/s00382-009-0641-5
- Burn, D. H., & Elnur, M. A. H. (2002). Detection of hydrological trends and variability. Journal of Hydrology, 255(1-4), 107–122. https://doi.org/10.1016/S0022-1694(01)00514-5
- BMD (2021). Bangladesh Meteorological Department.
- Chattopadhyay, S. & Edwards, D. R. (2016). Long-Term Trend Analysis of Precipitation and Air Temperature for Kentucky, United States. Climate, 4(1), 10. https://doi.org/10.3390/cli4010010
- Chittagong Division Topographic map. (2024). https://en-us.topographic-map.com/map-mgfcz4/Chittagong-Division/)
- Cong, R., & Brady, M. (2012). The Interdependence between Rainfall and Temperature: Copula Analyses. The Scientific World Journal, 405675. https://doi.org/10.1100/2012/405675
- Dash, S. K., Shekhar, M. S., & Singh, G. P. (2006). Simulation of Indian summer monsoon circulation and rainfall using RegCM3. Theoretical Applied Climatology, 86, 161–172. https://doi.org/10.1007/s00704-006-0204-1
- Deka, R. L., Mahanta, C., & Nath, K. K. (2019). Trends and Fluctuations of Temperature Regime of North East India. ISPRS Archives XXXVIII-8/W3 Workshop Proceedings: Impact of Climate Change on Agriculture, SAC, Ahmedabad, India, 376–380.
- Dore, M. H. I. (2005). Climate change and changes in global precipitation patterns: what do we know? Environment International, 31(8), 1167–1181. https://doi.org/10.1016/j.envint.2005.03.004

- Falga, R., & Wang, C. (2022). The rise of Indian summer monsoon precipitation extremes and its correlation with long-term changes of climate and anthropogenic factors. Scientific Reports, 12(1), 11985. https://doi.org/10.1038/s41598-022-16240-0
- Frimpong, B. F., Koranteng, A. & Molkenthin, F. (2022). Analysis of temperature variability utilising Mann–Kendall and Sen's slope estimator tests in the Accra and Kumasi Metropolises in Ghana. Environmental System Research, 11, 24. https://doi.org/10.1186/s40068-022-00269-1
- Gümüş, V., Soydan, N. G., Şimşek, O., Algin, H. M., Aköz, M. S., & Yenigun, K. (2017). Seasonal and annual trend analysis of meteorological data in Sanliurfa, Turkey. European Water, 59, 131–136.
- Ghumann, U., & Horney, J. (2016). Characterizing the impact of extreme heat on mortality, Karachi, Pakistan, June 2015. Prehospital and Disaster Medicine, 31(3), 263–266. https://doi.org/10.1017/S1049023X16000273.
- Gill, S. E., Handley, J. F., Ennos, A. R., & Pauleit, S. (2007). Adapting cities for climate change: the role of the green infrastructure. Built environment, 33(1), 115–133. https://doi.org/10.2148/benv.33.1.115
- Hossain, M. S. (2001). Biological aspects of the coastal and marine environment of Bangladesh. Ocean & Coastal Management, 44(3-4), 261–282. https://doi.org/10.1016/S0964-5691(01)00049-7
- Islam, I., Tonny, K. F., Hoque, M. Z., Abdullah, H. M., Khan, B. M., Islam, K. H. S., Prodhan, F. A., Ahmed, M., Mohana N. T., & Ferdush, J. (2024). Monitoring and prediction of land use land cover change of Chittagong Metropolitan City by CA-ANN model. International Journal of Environmental Science and Technology, 21, 6275–6286 (2024). https://doi.org/10.1007/s13762-023-05436-0
- Jones, B., O'Neill, B. C., McDaniel, L., McGinnis, S., Mearns, L. O., & Tebaldi, C. (2015). Future population exposure to US heat extremes. Nature Climate Change, 5, 652–655. https://doi.org/10.1038/nclimate2631
- Kahya, E., & Kalaychi, S. (2004). Trend analysis of streamflow in Turkey. Journal of Hydrology, 289, 128–144. https://10.1016/j.jhydrol.2003.11.006
- Kawser, U., Nath, B., Hoque, A. (2022). Observing the influences of climatic and environmental variability over soil salinity changes in the Noakhali Coastal Regions of Bangladesh using geospatial and statistical techniques. Environmental Challenges, 6, 100429. https://doi.org/10.1016/j.envc.2021.100429

- Kayano, M. T., & Sansígolo, C. (2009). Interannual to decadal variations of precipitation and daily maximum and daily minimum temperatures in southern Brazil. Theoretical and Applied Climatology 97, 81–90. https://doi.org/10.1007/s00704-008-0050-4
- Kendall, M. G. (1975). Rank correlation methods. Griffin, London.
- Khan, M. H. R., Rahman, A., Luo, C., Kumar, S., Islam, G. M. A., Hossain, M. A. (2019). Detection of changes and trends in climatic variables in Bangladesh during 1988–2017. Heliyon, 5(3), e01268. https://doi.org/10.1016/j.heliyon.2019.e01268
- Kodra, E., Steinhaeuser, K. & Ganguly, A. R. (2011). Persisting cold extremes under 21stcentury warming scenarios. Geophysical Research Letters, 38(8), L08705. https://doi.org/10.1029/2011GL047103
- Kottek, M., Grieser, J., Beck, C., Rudolf, B., & Rubel, F. (2006). World Map of the Köppen-Geiger climate classification updated. Meteorologische Zeitschrift, 15(3), 259–263. https://doi.org/10.1127/0941-2948/2006/0130
- Lambert, F., Stott, P., & Allen, M. (2003). Detection and attribution of changes in global terrestrial precipitation. Geophysical Research Letters, 5, 06140, https://doi.org/10.2307/1907187
- Mann, H. B. (1945). Nonparametric tests against trend. Econometrica, 13(3), 245–259. https://doi.org/10.2307/1907187
- Meehl, G. A., & Tebaldi, C. (2004). More intense, more frequent, and longer lasting heat waves in the 21st century. Science, 305(5686), 994–997. https://doi.org/10.1126/science.1098704
- Mishra, A. K. (2019). Quantifying the impact of global warming on precipitation patterns in India. Meteorological Applications, 26, 153–160. https://doi.org/10.1002/met.1749
- Norton, B. A., Coutts, A. M., Livesley, S. J., Harris, R. J., Hunter, A. M., & Williams, N. S. G. (2015). Planning for cooler cities: A framework to prioritise green infrastructure to mitigate high temperatures in urban landscapes. Landscape and Urban Planning, 134, 127–138. https://doi.org/10.1016/j.landurbplan.2014.10.018
- Nyembo, L. O., Larbi, I., & Rwiza, M. J. (2021). Analysis of spatiotemporal climate variability of a shallow lake catchment in Tanzania. Journal of Water and Climate Change, 12(2), 469–483. https://doi.org/10.2166/wcc.2020.197
- Pamarthi, A. (2020). The recent trend of the temperature in major cities of India: A difference between inland areas and coastal areas in the climate change scenario. Atmospheric Science, 1(1), 1–15.



- Pathirana, A., Denekew, H. B., Veerbeek, W., Zevenbergen, C., & Banda, A. T. (2014). Impact of urban growth-driven landuse change on microclimate and extreme precipitation A sensitivity study, Atmospheric Research, 138, 59–72, https://doi.org/10.1016/j.atmosres.2013.10.005
- Rahman, M. R., Salehin, M., & Matsumoto, J. (1997). Trend of monsoon rainfall pattern in Bangladesh. Bangladesh Journal of Water Resources, 14–18, 121–138.
- Roy, M., Biswas, B., & Ghosh, S. (2015). Trend analysis of Climate Change in Chittagong Station in Bangladesh. International Letters of Natural Sciences, 47, 42–53. https://doi.org/10.56431/p-7v90xn
- Sen, P. K. (1968). Estimates of the regression coefficient based on Kendall's tau. Journal of the American Statistical Association, 63(324), 1379–1389. https://doi.org/10.1080/01621 459.1968.10480934
- Shahid, S. (2010). Recent trends in the climate of Bangladesh. Climate Research, 42(3), 185–193, https://www.jstor.org/stable/10.2307/24870334
- Sudarsan, G., & Lasitha, A. (2023). Rainfall Trend analysis using Mann-Kendall and Sen's slope test estimation A case study. E3S Web of Conferences 405, 2023 International Conference on Sustainable Technologies in Civil and Environmental Engineering (ICSTCE 2023), 04013, 8. https://doi.org/10.1051/e3sconf/202340504013
- Sunny, F., Miah, M. S., Mia, M. Y., & Rimi, R. H. (2020). Temporal variability, trends of climatic variables and drought analysis of Rajshahi and Sylhet District, Bangladesh. Climate Research, Journal of the Asiatic Society of Bangladesh, Science, 46(2), 133–141. https://doi.org/10.3329/jasbs.v46i2.54409
- Tong, Y., Yu, Y., Hu, X., & He, L. (2015). Performance analysis of different kriging interpolation methods based on air quality index in Wuhan, 2015 Sixth International Conference on Intelligent Control and Information Processing (ICICIP), Wuhan, China, 331-335. https://doi.org/10.1109/ICICIP.2015.7388192
- Umer, Y., Jetten, V., Ettema, J., & Steeneveld, G. J. (2023). Assessing the Impact of the Urban Landscape on Extreme Rainfall Characteristics Triggering Flood Hazards. Hydrology, 10(1), 15. https://doi.org/10.3390/hydrology10010015
- Willett, K. M., Gillett, N. P., Jones, P.D., & Thorne, P. W. (2007). Attribution of observed surface humidity changes to human influence. Nature, 449, 710–712. https://doi.org/10.1038/nature06207
- Zhao, L., Lee, X., Smith, R. B., & Oleson, K. (2014). Strong contributions of local background climate to urban heat islands. Nature, 511, 216–219. https://doi.org/10.1038/nature13462